Zeitschrift: Schweizerische mineralogische und petrographische Mitteilungen = Bulletin suisse de minéralogie et pétrographie

Band: 80 (2000)

Heft: 2

Artikel: The relationships between the Kübler index, Weaver index and Weber index of illite crystallinity and their applications

Autor: Wang, Hejing / Zhou, Jian

DOI: https://doi.org/10.5169/seals-60960

SCHWEIZ. MINERAL. PETROGR. MITT. 80, 187–198, 2000

The relationships between the Kübler index, Weaver index and Weber index of illite crystallinity and their applications

by *Hejing Wang*[1] and *Jian Zhou*[2]

Abstract

Based on the distribution characteristics of the 10 Å XRD profile, fourteen equations relating the Kübler index, Weaver index and Weber index were derived. Four typical applications of these equations were developed in: (i) anchizone boundaries conversion; (ii) approximate illite domain size calculation for the Weaver index and Weber index; (iii) peak profile analysis and qualitative lattice strain/domain size evaluation; (iv) identification of the presence of illite/smectite from XRD profile in air-dried state.

From these relationships, a rapid and convenient method called the "KI–Wv Plot" for the estimation of strain/size and the identification of the presence of I/S in air-dried state is proposed. Influences on the KI–Wv plot method caused by variations in peak asymmetry, counting statistics and I/S are discussed. Both KISCH (1991) and WARR and RICE (1994) IC sets were tested with these relationships and with the method proposed. Comparisons with previous assessments of these relationships with the equations proposed suggests that BLENKINSOP's (1988) formulae show large variations and the "power law" between the Weaver index and Weber index reflects Lorentzian distribution across the illite 10 Å peak.

Keywords: illite crystallinity, IC indices, domain size, lattice strain, mixed layer, illite/smectite.

Introduction

The Weaver index (WEAVER, 1960), the Kübler index (KÜBLER, 1964) and the Weber index (WEBER, 1972) are indices of illite crystallinity and used by many researchers for studies of low grade metamorphism and basin maturity. Although the line broadening caused by lattice strain also contributes to the XRD profile (e.g. DRITS et al., 1998; JIANG et al., 1997), some of these indices of illite crystallinity are still convenient, useful and comparable methods for measuring profile changes in crystallinities and crystallite thickness (FREY, 1987; BLENKINSOP, 1988; MERRIMAN and PEACOR, 1999). For example, the Kübler index measures the half-height width of the 10 Å illite reflection and values decrease as peaks get narrower since the illite crystallites thicken in prograde metapelitic sequences. According to SCHERRER (1918) any half-height width of an XRD peak (i.e. the Kübler index where the 10 Å illite peak is considered) is directly proportional to the product of constant K and the wave length used and inversely proportional to the product of mean domain size and cosine theta. Hence, the Kübler index is directly linked with the Scherrer equation and thereby has a sound basis in crystallography, and hence is the most widely used. The Weaver index was the first proposed index of illite crystallinity (WEAVER, 1960). It measures the ratio of the height of the 10 Å reflection to that of the reflection at 10.5 Å and values increase as the peak becomes narrower. However it is difficult to relate the Weaver index to any changes in crystallographic parameters. The Weber index expresses the half-height width of the 10 Å illite reflection as a ratio to the width of the (100) peak of a quartz standard and values decrease as peaks become narrower. It makes IC values comparable when different laboratories use the same quartz standard. However, it is not directly connected to the Scherrer equation. In order to compare the boundaries of anchizone for both Kübler index and Weaver index, KÜBLER (1968) plotted an approximately inverse curve with more than 700 pairs of values of the Kübler index and Weaver

[1] Department of Geology, Peking University, Beijing 100871, China. <hjwang@pku.edu.cn>
[2] Chinese Academy of Geology, 26 Baiwanzhuang, Beijing 100037, China.

index from which the anchizone boundaries of the Kübler index were allowed to be set as 7.5–4 mm or 0.56–0.3 °Δ2θ from the Weaver index limits 2.3–12.1 (KÜBLER 1968, Fig. 3). This figure actually describes the general relationship between the Kübler index and Weaver index, although there is no mathematical expression. BLENKINSOP (1988) tested the relationships between Kübler index, Weaver index and Weber index by fitting mathematical functions to each pair of indices measured from the same sample. He proposed that an exponential law or power law related the Kübler index and Weaver index, a power law related the Weber index and Weaver index, and a linear law existed between the Kübler index and Weber index. However, there are still some problems with these IC indices. For example, it seems, as described above, that the Weaver index and the Weber index lack a sound basis in crystallography. Moreover, the relationships proposed by BLENKINSOP (1988) are still uncertain because of (1) errors produced from the measurement, (2) the interference of other phyllosilicates (FREY, 1987), and (3) the change in shape of the 10 Å peak. The main purpose of this paper is to establish the mathematical relationships between the three indices of IC and hence, to establish the crystallographic basis for the Weaver and Weber indices. In addition we shall explore new applications for these indices and their mathematical relationships.

Relationships between Kübler index, Weaver index and Weber index

Usually an XRD peak possesses the following defined properties: a certain position in Bragg diffraction angle, a certain height, a certain width, sharp or smoothed top with broad or narrow bottom, tailing on one side or symmetrical. These properties were summarised as five basic parameters and two additional parameters of an XRD reflection by WANG and ZHOU (1998) and each of them contains its own physical meaning such as: the peak position reflects the d-spacing of a hkl plane, the width describes changes in crystallinity of the crystallites and so on. Since the mathematical functions can very well describe these characteristics of an XRD peak (for example, in the Gaussian function I_{max}, B, x and the variation of B in two sides stand for the maximum, half width, difference from the position and the asymmetry, the Gaussian function itself represents the special distribution or the shape of the peak, see later) they have been widely used in X-ray diffractometry for more than sixty years (JONES, 1938; RIETVELD, 1969; LONGFORD 1978; BALZAR and POPOVIC, 1996). Extensive use of mathematical functions to describe XRD profiles and to study crystallographic problems have been documented. For example the well known "Rietveld method" uses mathematical functions to fit profiles for structure refinement and now is very widely applied. Some 341 papers used the Rietveld method or referred to it during the period between January 1987 to May 1989 (RIETVELD, 1993). According to

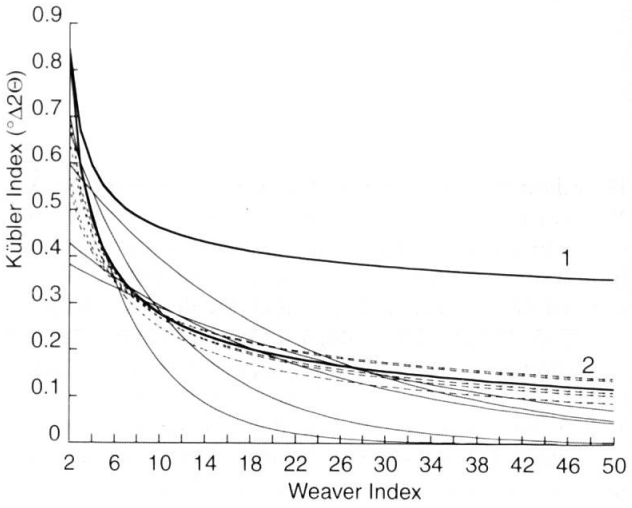

Fig. 1 Relationship between Kübler index and Weaver index. Thick solid line 1 is from equation (1) or (2) and thick solid line 2 from equation (3) or (4). Thin solid lines are from BLENKINSOP's (1988) empirical formulae of "exponential law" and dashed lines are from the "power law".

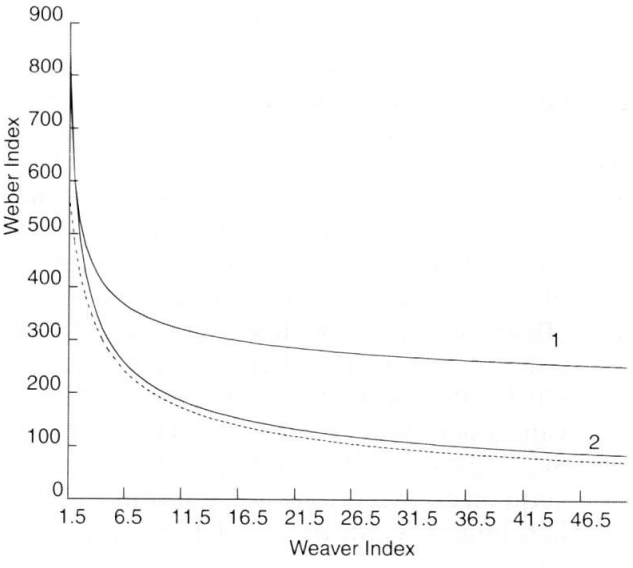

Fig. 2 Relationship between Weaver index and Weber index. Solid lines 1 and 2 are from equations (7) or (8) and (9) or (10) respectively. Dashed line is from BLENKINSOP's (1988) empirical formula.

the ISI citation database, 211 papers published in two journals, *Journal of Applied Crystallography* and *Powder Diffraction*, used mathematical functions for XRD profile analyses, other than the Rietveld method, between January 1973 and June 1999. These mathematical functions are also installed in modern diffractometers, such as the Siemens D500, D5000, Rikagu Dmax/2000, 2400 and BD90. Therefore the use of mathematical functions to model the XRD profile is an advanced and credible modern theoretical method. However, scientifically, we still assume that the 10 Å XRD peak profiles possess the characteristics of Gaussian and Lorentzian distributions as the two extremes and the Pearson (VII) distribution as the intermediate component (HOWARD and PRESTON, 1989).

Tab. 1 Contents and detail information of constants C_1 to C_{14}.

Constants	*Content*	*Note*
C_1	$2x(\ln 2)^{0.5}$	$x = 0.422\ \Delta°2\theta$, CuK$\alpha$
C_2	$\exp(C_1^2)$	
C_3	$2x$	
C_4	C_3^2	
C_5	$2x\,(2^{1/u}-1)^{0.5}$	$u = 1 \sim \infty$
C_6	C_5^2	
C_7	$C_1\,C_{14}$	
C_8	$C_2\,C_{14}^2$	
C_9	$C_3\,C_{14}$	
C_{10}	$C_4\,(C_{14})^2$	
C_{11}	$C_5\,C_{14}$	
C_{12}	$C_6\,(C_{14})^2$	
C_{13}	$1/C_{14}$	
C_{14}	$100/B_{100}^{Q}$	$B_{100}^{Q} = 0.14\ °2\theta$

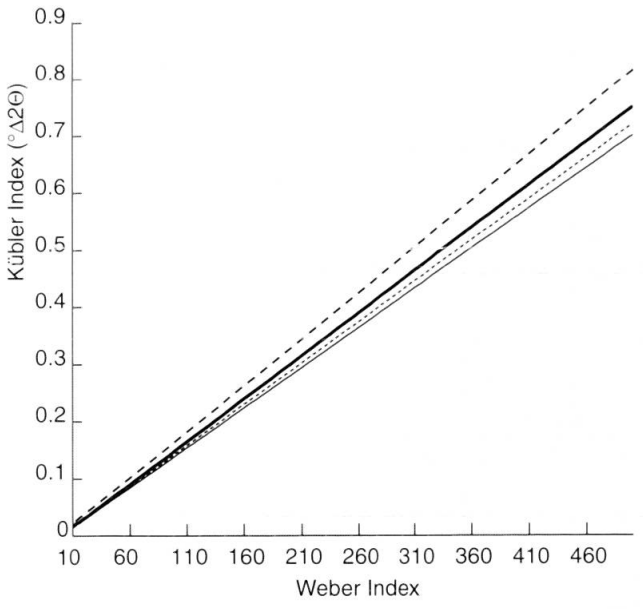

Fig. 3 Relationship between Kübler index and Weber index. Thick solid line, thick dashed line, thin dashed line and thin solid line are from WEBER (1972), LUDWIG (1972), BLENKINSOP (1988) and equation (13) or (14).

Using these definitions of the three indices of IC, and three functions to model the 10 Å reflection of illite, carefully working through each step, the following relationships between the Kübler index, Weaver index and Weber index of IC were obtained:

The relationships between Kübler index (KI) and Weaver index (Wv) is given for the Gaussian curve by:

$$KI = C_1 / (\ln Wv)^{1/2} \quad (1)$$

$$Wv = (C_2)^{KI^{-2}} \quad (2)$$

for the Lorentzian curve by:

$$KI = C_3 / (Wv - 1)^{1/2} \quad (3)$$

$$Wv = C_4\,KI^{-2} + 1 \quad (4)$$

for the Pearson (VII) curve by:

$$KI = C_5 / (Wv^{1/u} - 1)^{1/2},\ u = 1 \sim \infty$$

$$Wv = (1 + C_6\,KI^{-2})^{u},\quad u = 1 \sim \infty \quad (6)$$

where C_1, C_2, C_3, C_4, C_5 and C_6 are constants and their values are listed in table 1. Figure 1 is a plot of the six equations and is called the KI–Wv plot.

The relationships between the Weaver index (Wv) and Weber index (Wb) are given for the Gaussian curves by:

$$Wb = C_7 / \ln Wv)^{1/2} \quad (7)$$

$$Wv = (C_8)^{Wb^{-2}} \quad (8)$$

for the Lorentzian curve by:

$$Wb = C_9 / (Wv - 1)^{1/2} \quad (9)$$

$$Wv = C_{10}\,Wb^{-2} + 1 \quad (10)$$

for the Pearson (VII) curve by:

$$Wb = C_{11} / (Wv^{1/u} - 1)^{1/2} \quad (11)$$

$$Wv = (1 + C_{12}\,Wb^{-2})^{u} \quad (12)$$

where C_7, C_8, C_9, C_{10}, C_{11} and C_{12} are constants and their values are listed in table 1. Figure 2 is a plot of equations 7–12.

The relationships between the Kübler index (KI) and Weber index (Wb) are given by:

$$KI = C_{13}\,Wb \quad (13)$$

$$Wb = C_{14}\,KI \quad (14)$$

where C_{13}, C_{14} are constants and their values are listed in table 1. Figure 3 is a plot of equations 13 and 14.

By viewing the relationships between equations 1–14, the following deductions can be made. Generally for the Gaussian curve the 10 Å peak of illite can be expressed as:

$$I_i = I_{\max} \exp\,[-\ln 2\,(x_i / B)^2] \quad (15)$$

where $I_{\max}$ is the maximum intensity of the 10 Å reflection, B stands for the full width at half maximum or the Kübler index KI, x_i denotes the difference (in °2θ) between a chosen intensity point I_i and the maximum. Hence the intensity at 10.5 Å ($I_{10.5}$) of the 10 Å reflection of illite in the Gaussian distribution is expressed as:

$$I_{10.5} = I_{\max} \exp\,[-(2x_{10.5} / B)^2 \ln 2]. \quad (16)$$

Tab. 2 Comparison of the measured IC values (Wv, KI and Wb) with those calculated from equations 3, 4, 9, 10, 13 and 14 for the IC sets of WARR and RICE (1994) and KISCH (1991).

Sample of IC set	Measured with BD86-90	Predicted from equations 3, 4, 9, 10, 13 and 14	Error of Wv (%)	Comment
SW1 air-dried	KI=0.396 Wv=3.56 Wb=283	Wv=5.54; Wb=283 KI=0.53; Wb=377 KI=0.396; Wv=5.54	35.74	AS=1.25, I/S present
SW1 EG treated	KI=0.353 Wv=5.26 Wb=252	Wv=6.72;Wb=252 KI=0.409; Wb=292 KI=0.353; Wv=6.72	21.73	AS=0.88, 001/001 and 001/002 of I/S present
SW2 air-dried	KI=0.354 Wv=4.50 Wb=253	Wv=6.68; Wb=253 KI=0.451; Wb=322 KI=0.354; Wv=6.68	32.63	AS=1.42, I/S present
SW2 EG treated	KI=0.329 Wv=5.86 Wb=235	Wv=7.58;Wb=235 KI=0.383; Wb=273 KI=0.329; Wv=7.58	22.69	AS=1.07, 001/001 and 001/002 of I/S present
SW4 air-dried	KI=0.277 Wv=9.08 Wb=198	Wv=10.28; Wb=198 KI=0.297; Wb=212 KI=0.277; Wv=10.28	1.32	AS=1.10, I/S present
SW4 EG treated	KI=0.267 Wv=12.02 Wb=191	Wv=10.99; Wb=191 KI=0.254; Wb=182 KI=0.267; Wv=10.99	-9.37	AS=0.99, 001/001 and 001/002 of I/S present
SW6 air-dried	KI=0.184 Wv=34.90 Wb=131	Wv=22.04; Wb=131 KI=0.145; Wb=104 KI=0.184; Wv=22.04	-58.3	AS=1.18, u=1.412
SW6 EG treated	KI=0.183 Wv=37.97 Wb=131	Wv=22.27; Wb=131 KI=0.139; Wb=99 KI=0.183; Wv=22.27	-70.5	AS=1.12
FM1c crystal	KI=0.07 Wv= - Wb=50	Wv=146; Wb=50 KI=0.07; Wv=146	-	AS=0.87
kap8041 rock chip	KI=0.395 Wv=3.07 Wb=282	Wv=5.56; Wb=282 KI=0.587;Wb=419 KI=0.395; Wv=5.56	44.78	AS=3.80, *K-illite and NH_3-illite present
kn9226 rock chip	KI=0.226 Wv=9.30 Wb=161	Wv=14.95; Wb=161 KI=0.293; Wb=209 KI=0.226; Wv=14.95	37.79	AS=1.57
kn7559 rock chip	KI=0.224 Wv=8.17 Wb=160	Wv=15.20; Wb=160 KI=0.315; Wb=225 KI=0.224; Wv=15.20	46.25	AS=1.61
kn9213 rock chip	KI=0.204 Wv=18.79 Wb=146	Wv=18.12; Wb=146 KI=0.200; Wb=143 KI=0.204; Wv=18.12	-3.70	AS=1.42
kn7547 rock chip	KI=0.168 Wv=59.31 Wb=120	Wv=26.24; Wb=120 KI=0.111; Wb=78.95 KI=0.168; Wv=26.24	-126	AS=1.26
kn7513 rock chip	KI=0.162 Wv=54.76 Wb=116	Wv=28.14; Wb=116 KI=.115; Wb=82.22 KI=0.162; Wv=28.14	-94.6	AS=1.18, u=1.769

* KISCH (1996) private communication.
The correlation of IC results with Kisch IC set is:
IC (this work) = 0.8297 × IC KISCH (1991) – 0.0006 $R^2 = 0.98$
and that with WARR and RICE (1994) IC set is:
IC (this work) = 0.6475 × IC WARR and RICE (1994) – 0.0175 $R^2 = 0.97$
AS is the asymmetric parameter of an XRD peak (see Fig. 8).
u is the exponent of the Pearson VII function.

By moving I_{max} to the left hand side, the expression becomes that of the Weaver index ($I_{max}/I_{10.5}$), hence equation 16 becomes:

$$I_{max} / I_{10.5} = \exp [(2x_{10.5} / B)^2 \ln 2]. \quad (17)$$

By replacing $I_{max}/I_{10.5}$ with Wv, and B with the Kübler index KI, equation 17 becomes:

$$Wv = \exp [(2x_{10.5} / KI)^2 \ln 2] \quad (18)$$

This is equation 2: $Wv = \{\exp [(2x_{10.5})^2 \ln 2] \}^{KI^{-2}}$, and hence $C2 = \exp [(2x_{10.5})^2 \ln 2]$.
From equation 18 it is easy to rewrite equation 1:

$$KI = 2x_{10.5} (\ln 2)^{1/2} / [\ln (Wv)]^{1/2} \text{ and thereby}$$

$$C_1 = 2x_{10.5} (\ln 2)^{1/2}.$$

Similarly from the general expressions of intensity at 10.5 Å of the 10 Å illite reflection in the Lorentzian and Pearson (VII) distributions:

$$I_{10.5} = I_{max} / [1 + (2x_{10.5} / B)^2], \quad (19)$$
$$I_{10.5} = I_{max} / [1 + (2^{1/u} - 1) (2x_{10.5} / B)^2]^{-u} \quad (20)$$

The constants C_{3-6} can be deduced, whereas C_{13} and C_{14} are obtained directly from the definition of the Weber index. Inserting C_{14} into equations 1 to 6 and comparing with equations 9 to 12, the constants C_7 to C_{12} may also be obtained.

Assessment of relationships by actual measurement

In order to evaluate the practical application of the proposed equations, the three measured IC indices from both the KISCH (1991) and the WARR and RICE (1994) set of IC standards were compared with those predicted from these relationships. The procedure of sample preparation for the Warr and Rice IC standards were followed using the recommendations of the IGCP 294 IC working group (KISCH, 1991). A BD86 diffractometer with external data managing system was run at 30 kV and 30 mA, CuKα, 1° divergence slit and 0.4 mm –1° receiving slits, no monochromator and a time constant of 1 s, 1°/min scanning speed and 0.02° scanning step. $K\alpha_2$ wavelength was not stripped. The background was properly subtracted from the measured profiles. A smoothing operation was performed within 9 points polynomial (SAVITZKY and GOLAY, 1964) in order to avoid additional broadening.

The Kübler index was measured by the full width at half maximum intensity (FWHM) of the 10 Å illite reflection. The Weber index was calculated from the ratio of the FWHM of the 10 Å illite reflection to that of the quartz (100) peak. The ratio of the height at 10 Å to that at 10.5 Å of the first illite basal reflection was treated as the Weaver index. When the first illite basal reflection shifts slightly away from 10 Å this ratio was calculated using the height at the maximum to that at the position of the maximum plus 0.5 Å (or maximum minus 0.422 °Δ2θ for CuKα radiation). From the results listed in table 2 it seems that, for both the WARR and RICE (1994) and the KISCH (1991) IC set, that measured values of the Kübler index coincided well with those predicated by Weber index values, but not with predicated Weaver index values. The former case is because the width of the (100) reflection of standard quartz is fixed and hence the only variable is the width of the first illite basal reflection. The inaccuracy in the latter is because of asymmetry in the first illite basal reflection peaks (see AS ≠ 1), the presence or the interference of illite/smectite (I/S) and other phases (NH_3-illite on K-illite, for instance), the influence of a certain strain (see next two sections) and errors associated with measurement.

Applications

According to the relationships proposed above we can convert the IC value of one index into another. Therefore the first application of these relationships is to convert the boundaries of the anchizone from one index into the other two. Since one of these line broadening analyses is based on the assumption that the Gaussian distribution in an XRD peak is attributed to the lattice strain and

Tab. 3 The anchizone boundaries derived from equations 3, 9, 4, 14, 13 and 10. The boundary values in bold are original values, those in ordinary printface being derived values, those in italic are derived from BLENKINSOP (1988), equations 1, 2 and 3.

Sources	Weaver index Wv	Kübler index KI in ° Δ2θ	Weber index Wb
WEAVER (1960)	**2.3–12.1**	0.74–0.25 *0.64–0.24*	529–181 *446–167*
KÜBLER (1967)	5.0–12.4 *4.7–11.4*	**0.42–0.25**	300–179 *292–174*
WEBER (1972)	16.1–17.2 ~ 31.0–34.0 *13.8–14.6 ~ 24.7–26.7*	0.22–0.21 ~ 0.15 *0.22 ~ 0.16–0.15*	**155–150 ~ 110–105**

the Lorentzian distribution to the domain size, the Lorentzian relationships equations 3, 4, 9, 10 and 13, 14 were used to calculate the anchizone boundaries of the three indices related to the particle size. Table 3 gives values of anchizone boundary derived from these equations, the values from BLENKINSOP (1988) are also listed for comparison. The illite crystallinity concept has been widely applied and has a sound theoretical foundation and an extensive set of experimental results (e.g., WARREN and AVERBACH, 1952; WARREN, 1959; SCHOENING, 1965; RULAND, 1968; KLUG and ALEXANDER, 1974; LANGFORD, 1978; NANDI and SEN GUPTA, 1978; JONES, 1981; LANGFORD et al., 1986; LANGFORD, 1992; BALZAR and LEDBETTER, 1993; DELHEZ et al., 1993; BALZAR and POPOVIC, 1996).

The second application of these relationships is to calculate the approximate domain size of illite from the IC values of the Weaver and Weber indices. That is, from equations 3 and 13, the IC values of the Weaver index and the Weber index can be converted into values of FWHM (the Kübler index) and then, with the Scherrer equation, the approximate mean domain size of illite can be derived. For example, the IC value of 34.9 from the Weaver index of IC set SW6 air-dried measured, 0.145 °$\Delta 2\theta$ is an equivalent value of FWHM. From the Scherrer equation the mean domain size of illite in SW6 is given as 550 Å under the conditions of CuKα radiation, 8.8 °2θ Bragg angle and 0.9 as the value of constant K. Note that in this example, 34.9 is not corrected with a correlation formula as information for the Weaver index of these IC sets is not available.

The third application of these relationships is lattice strain or domain size/lattice strain analysis. It is well known that line broadening is the result of two factors, the domain size and the lattice strain. Nowadays more and more attention is paid to the broadening caused by lattice strain since it could greatly influence IC studies and should not be neglected. As mentioned above the Gaussian distribution component of an XRD peak indicates the degree of lattice strain and the Lorentzian component describes the state of domain size. If it is possible to separate the component of strain broadening from the XRD profile we can evaluate the magnitude of pure broadening from coherent domain size. HALDER and WAGNER (1966) proposed a simplified formula to describe the relationship between integral breadth β of a line, the Gaussian integral breadth β_g and the Lorentzian integral breadth β_c:

$$\beta^2 = \beta_c \beta + \beta_g^2. \quad (21)$$

In this equation, the three peak parameters b, b_g and b_c are parabolically related. It shows that given the integral width of an XRD peak (note that b, b_g and b_c are all greater than zero), the greater the Gaussian component of the peak, the greater the lattice strain is. Detailed equations can be found in KLUG and ALEXANDER (1974). Equations 1 or 2 describe the Gaussian relationship between the Weaver and Kübler indices, equations 3 or 4 describe the Lorentzin relationship between the two indices and equations 5 or 6 describe the intermediate states. With these equations we can therefore evaluate the Gaussian component in a peak and hence analyse qualitatively the state of lattice strain on samples when their integral widths are equal or roughly the same.

Figure 4 (A–F) is a plot of these equations in which the uppermost curve is the 100% Gaussian (lattice strain) curve and the lowest curve is the 100% Lorentzian (domain size) curve and those in between the two extremes are curves with exponents being 1.5, 2, 3 and 5. The values of exponents are marked at the end of each curve. Increasing the exponent of Pearson VII from 1 to infinity transforms the Pearson VII curve from a Lorentzian distribution to a Gaussian distribution (i.e. the higher the exponent, the higher the Gaussian component). Then, any point falling on the lowest curve indicates no distortion in the lattice and these falling on the upmost curve denote peak broadening caused entirely by lattice strain. Consequently, those falling between the two extremes indicate peak broadening by both domain size and lattice strain. Therefore we name the area between the two extreme curves as "the size/strain region".

Equation 21 also suggests that the higher the integral width and the greater the Gaussian component of the 10 Å peak, the greater the lattice strain. It is surmised here that, on one hand, the higher the plotted point (broader peak) along the same exponent curve in figure 4 (A–F), the greater the lattice strain; on the other hand, the closer to the uppermost curve (higher *u* value) along the same integral width iso-curve, the higher the lattice strain. Therefore points plotting in the upper right corner in the "strain region" indicate a higher state of lattice strain than those in the lower left, whereas the domain sizes cases are *vice versa*. These iso-values are marked by the ends of iso-lines of integral width either along the Gaussian curve or along the Lorentzian curve in figure 4 (A–F).

The procedures for actual qualitative lattice strain analysis are: first, measure the IC values of the Kübler and Weaver indices for each sample carefully; secondly, plot the pairs of IC values of the two indices on figure 4 (A–F) according to the AS value measured from the higher anchizone or epizone; and then, the relative states of lattice

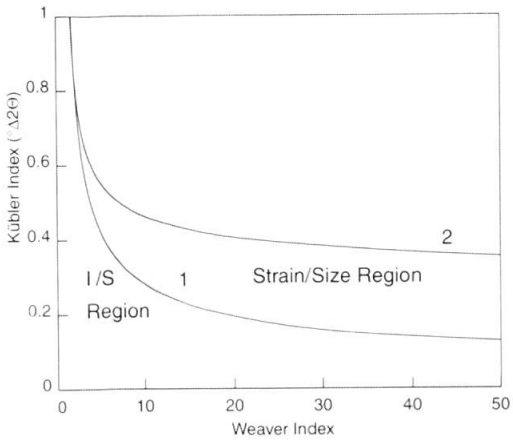

Fig. 4 Applications of the relationship between Kübler index and Weaver index. The area marked by "Strain/Size Region" indicates the peak breadth which are caused by both lattice strain and domain size. The area marked by "I/S Region" indicates the presence of I/S. Curve 1, dividing the two areas, suggests that peak breadth is the result of the domain size. Curve 2, as the upper boundary of the area "Strain/Size Region", denotes that the peak breadth is caused entirely by lattice strain.

(A–F) present the "Strain/Size Region" as detailed grids of iso-integral width and iso-exponents with different degrees of asymmetry AS = 1, 1.1, 1.2, 1.3, 1.4 and 1.5. The symmetrical Gaussian and Lorentzian curves are depicted by the pair of dashed lines for comparison. In figure 4C the filled circles are plotted from Warr and Rice's IC set and the filled triangles are from Kisch's IC set. See text for detail.

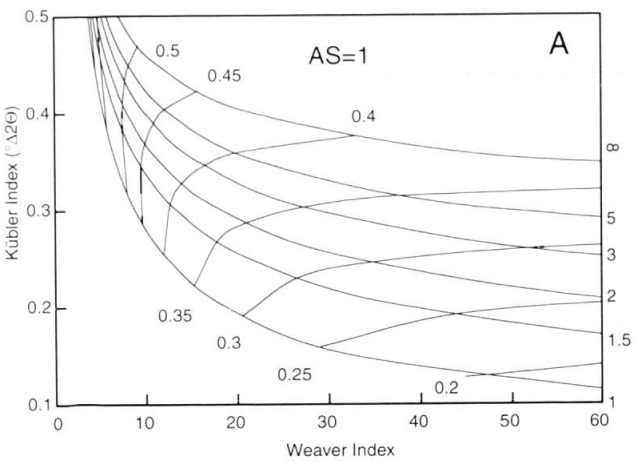

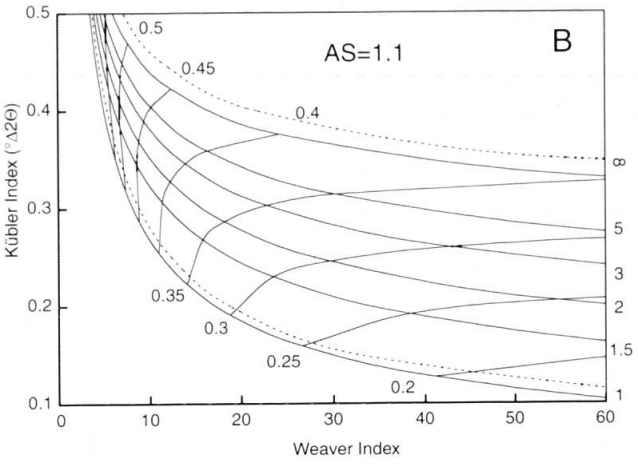

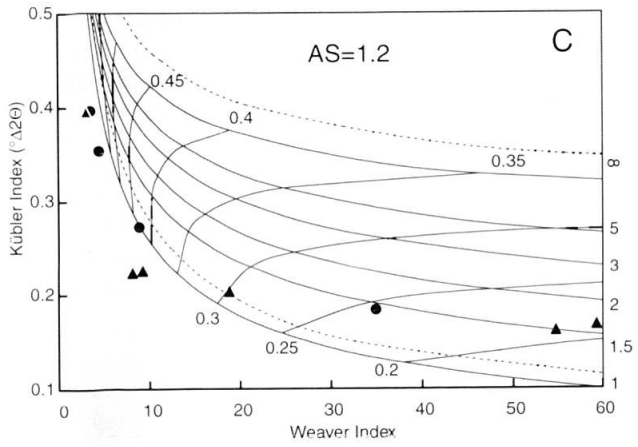

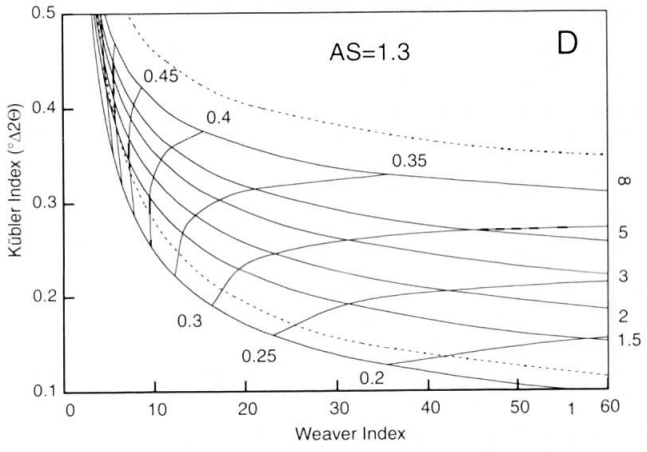

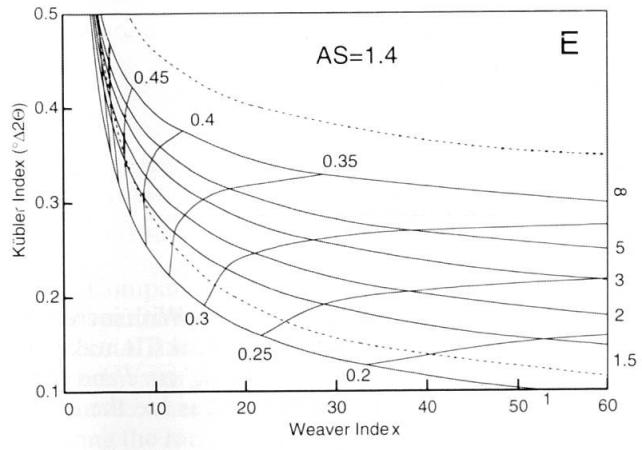

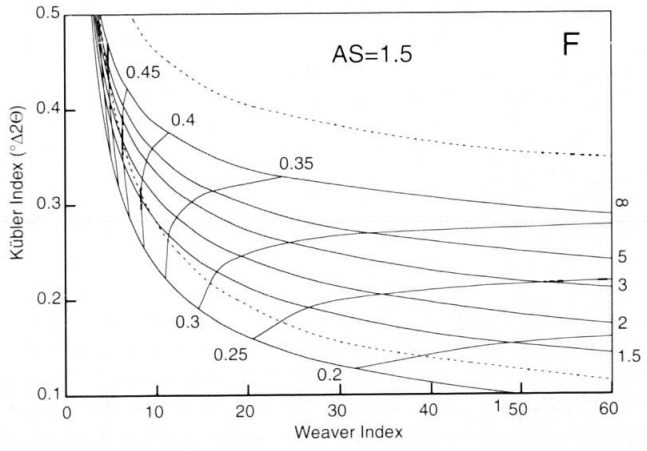

strain for samples may be read from the diagram. Both sets of IC standards, from KISCH (1991) and WARR and RICE (1994), are plotted in figure 4C from which Kn7547 and Kn7513 of Kisch and SW6 of Warr and Rice are in the strain/size region and SW6 is in a state of higher lattice strain than that of Kn7547 and Kn7513 since they fall on nearly the same exponent line ($u = 1.412$, AS = 1.18).

The fourth application is to evaluate the presence of mixed layer illite/smectite (I/S). Illite and mixed layer I/S commonly occur in rocks from the diagenetic zone and lower anchizone such as shales, marls, sandstones and limestones. Hence both illite and I/S reflections will be present in the XRD profiles of such samples, generating peaks around 6.5 to 12 °2θ in the XRD profile (Fig. 5). With increasing Reichweite (R) from 0 to 3 the d-spacing of I/S decreases from close to 15 Å to near 10 Å. In the case of I/S with R > 1 the d spacing of I/S is often less than 12 Å (WANG et al., 1996). Since the crystallinity of I/S is poor the peak of air-dried I/S in this segment is broad and hence

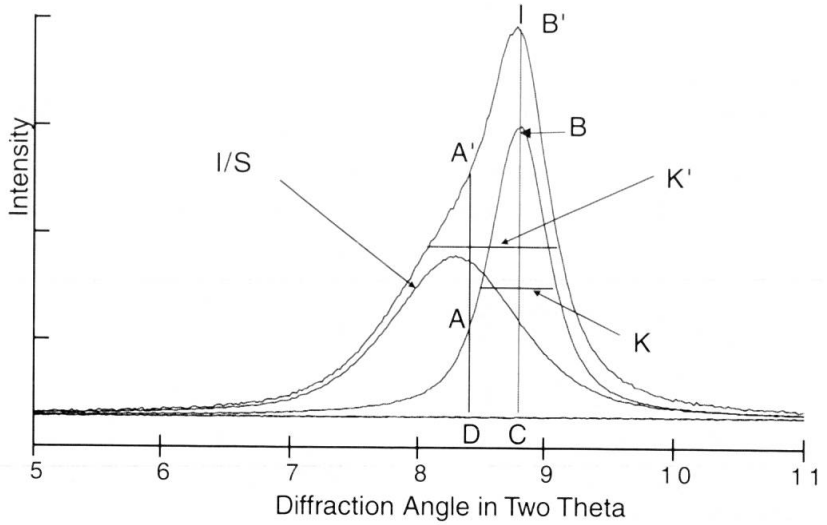

Fig. 5 Influence on the Weaver index and the Kübler index measurements of illite (I) as the result of the presence of mixed-layer illite/smectite (I/S). The height at maximum of the first illite basal reflection changes from CB to CB' and the height at 10.5 Å increases from AD to A'D while the half-width changes from K to K' due to the presence of illite/smectite. This, in most cases, results in the plot point of KI and Wv being outside the area "Strain/Size Region" and under curve 1 in figure 4.

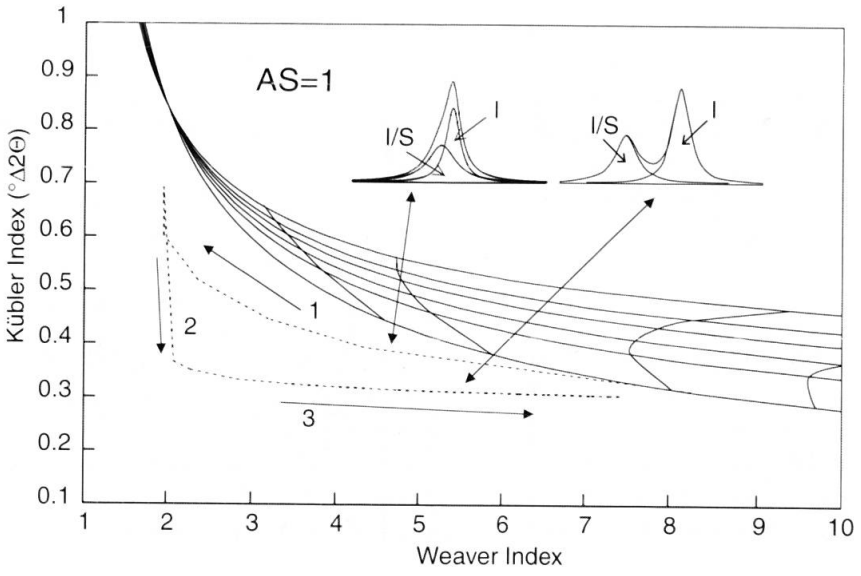

Fig. 6 Traces on KI–Wv plot resulting from the changes as a result of the increase in d-spacing in I/S. With increased d-spacing in I/S, the illite 10 Å peak alters from a convoluted asymmetric peak into two interfering peaks. It makes an approximate triangle trace (dotted line): trace 1 marks the "single peak" case, trace 3 the "two peak" case and trace 2 the transition case. Arrows indicate the direction of the increasing d-spacing in I/S. Inserted figures are the corresponding cases of I/S interfering with the illite 10 Å peak (I).

this I/S peak will interfere with the illite 10 Å peak and distort the IC values of both Kübler and Weaver indices. Generally the presence of I/S will increase the value of the Kübler index and decrease the value of the Weaver index (Fig. 6).

Theoretical analysis indicates that the presence of I/S will cause the plot of Wv and KI values to shift from the strain/size region into the area below (Figs 6 and 7). On the other hand, for those samples without I/S the first illite basal reflection is the only peak around 10 Å and there is a good relationship between the Kübler index and Weaver index. The plots for the two indices will fall in the "strain/size region" according to their strain states. This enables the presence of I/S in air-dried samples to be distinguished: values from regular IC data (no influence from I/S or no I/S) of the Kübler and Weaver indices will plot on these relationship curves whereas those from data containing I/S or influenced by I/S will plot under these

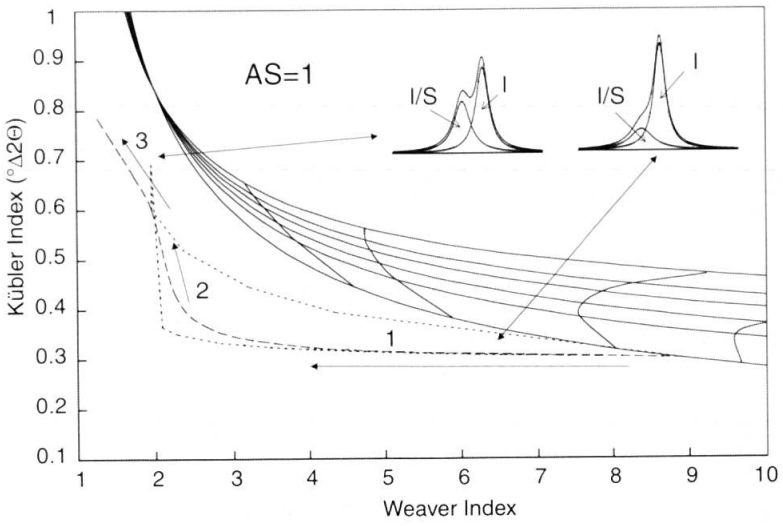

Fig. 7 Trace on KI–Wv plot from the changes resulting in increasing the amount of I/S. For an I/S with d-spacing near 10 Å, increasing the amount of I/S, the illite 10 Å peak alters from a convoluted asymmetric peak into two interfering peaks. It makes a deformed letter "Z" trace (dashed line): portion 1 marks the "single peak" case, portion 3 the "two peak" case and portion 2 the transition case. The trace of the increasing d-spacing of I/S is also given as dotted lines for comparison. Arrows indicate the direction of increasing amounts of I/S. Inserted figures are the corresponding cases of I/S interfering with the 10 Å illite peak (I).

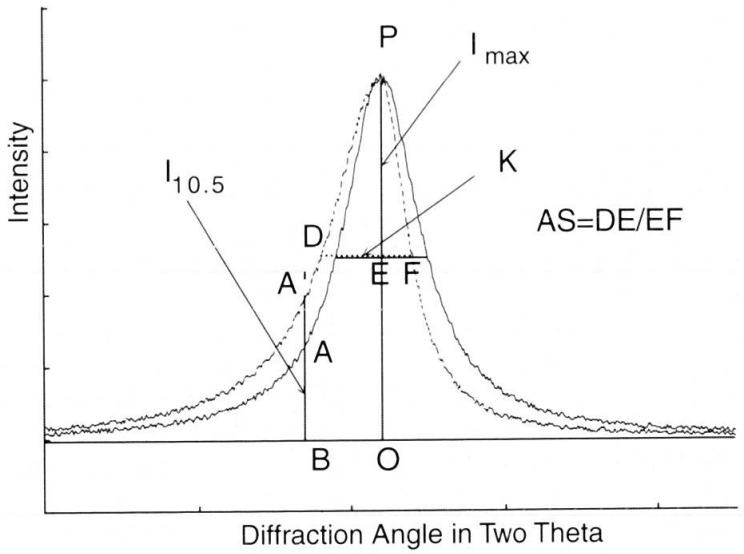

Fig. 8 Comparison of the Wv measurements from a symmetrical and asymmetrical peak with the same half-width. For the symmetrical peak (solid line) Wv ($I_{max}/I_{10.5}$) = PO/AB and for the asymmetrical peak (dashed line) Wv = PO/A'B; since A'B > AB, the asymmetrical peak's value of Wv is less than that of the symmetrical peak. It makes the plot of KI and Wv to shift to the lower Wv side than that of the symmetrical peak. To the contrary, the plot point will be above these curves when the peak becomes asymmetrical to the higher diffraction angle side. AS is the asymmetric parameter measuring the ratio of the width (DE) in lower diffraction angle side to that (EF) in higher diffraction angle side.

curves. Hence the area under the "strain/size region" is called as "I/S region". In figure 4 (A–F) any data points of the Kübler and Weaver indices falling in the "I/S region" indicate the presence of I/S, if the strain is weak and the measurement is correct with no interference from other reflections. Plots of the two IC sets indicate the presence of I/S in SW1, SW2, Kn7559 and Kn9226 or of NH_3-illite in Kap8041. SW4 plots just under the Lorentzian curve and indicates the presence of little I/S (Wv 9.08 measured is less than predicted 10.28; see Tab. 2). The results from SWs agree well with experimental values (see WARR and RICE, 1994). Calculated data for sample Kap8041 also agrees with measured values. There is no information on the I/S content of samples Kn9559 and Kn9226.

When figure 4 (A–F) is used to distinguish the presence of I/S and to analyse the state of lattice strain the following points need to be considered:

(1) Very careful measurement of the IC values of the Kübler and Weaver indices are critical especially when the peak is narrow.

(2) Utilisation of the asymmetric parameter (AS) from the sample of higher anchizone or epizone to chose the appropriate section of figure 4 (A–F). To measure the value of AS, draw a line though the maximum and measure, at the half maximum, the width on the lower diffraction angle side and on the higher diffraction angle side; the ratio of the width on the lower side to that on the higher side is the asymmetric parameter (Fig. 8). Note that the asymmetry of XRD peaks is characterised by several methods such as the half-width asymmetry, the shape asymmetry, the shape and half width asymmetry, vertical asymmetry and complex asymmetry (WANG and ZHOU, 1998). The half-width asymmetry is most commonly used.

(3)Use figures 4 B–F for asymmetric peaks according to the degree of asymmetry since the IC value of Wv decreases as AS increases (see Fig. 8).

(4) It is not necessary to correct the measured IC values of the Kübler index and Weaver index as it offers all information of the two indices and these parameters: maximum intensity, peak area, position and AS from the IC sets. It is wrong to use corrected Kübler index values with measured Weaver index values in the figures constructed. As KÜBLER (1968) pointed out, it is very difficult to measure the Wv from a narrow 10 Å peak, especially when the counting statistics are poor (KLUG and ALEXANDER, 1974). Therefore, for peaks falling in the very low (FWHM very small) I/S region it does not necessarily indicate the presence of I/S but possibly the incorrect measurement of Wv or perhaps the presence of another phase.

Discussion

Asymmetric effect: According to ALEXANDER (1948), XRD peak asymmetry is caused by the geometric conditions of diffraction and is observed as a tailing to low angles, especially at lower angles of diffraction. This will cause the Wv to decrease but has no effect on KI if the width of the XRD peak is only a function of domain size and lattice strain. When AS increases, Wv will decrease rapidly, this will cause Wv to shift to lower values on the curves in figure 4 than in the case for normal symmetrical peaks. Therefore one should carefully measure the degree of asymmetry (AS) when using figure 4 for domain size or lattice strain analyses.

Change in the KI–Wv plot related to I/S: The presence of I/S causes the value of the Kübler index to increase, the value of the Weaver index to decrease and plots of the two values to fall into the I/S area of figure 4. An increase in the d-spacing of I/S from close to 10 to nearer 15 Å (the Reichweite R decreasing from $R > 1$ to $R = 0$), causes an increase in KI, and a decrease in Wv so that the two values plot in the I/S region while the peak becomes asymmetrical and convoluted. With further increases in the d-spacing of I/S, the single asymmetrical peak begins to separate, thus KI decreases rapidly while Wv decreases very slowly. Further increases in the d-spacing of I/S causes peak separation and both KI and Wv approach the original values of the 10 Å peak, hence the influence of I/S on the 10 Å peak becomes progressively weaker. The resulting plot of KIs and Wvs is roughly a right-angle triangle: the "slope" is the trace of a single asymmetrical peak (a convolution of 10 Å peak and the peak of I/S), the "base" is the trace of two interfering peaks and the "vertical" is the trace of the transition from a single peak to two peaks (Fig. 7).

Fixing the d-spacing of I/S (d-spacing near 10 Å) and increasing the amount of I/S produces similar changes to the peak patterns as increasing the d-spacing of I/S (Fig. 8). However the traces of these changes are different. Initially, the increased amount of I/S is small and the influence of I/S on the 10 Å peak is weak; KI increases weakly or very weakly and Wv decreases rapidly for relatively narrow and narrow peaks and the peak appears as a single. Secondly, with a progressive increase in the amount of I/S, its peak maximum begins to emerge from the convoluted single peak, and KI increases relatively rapidly whereas the Wv decreases slowly. Finally, with further increases in the amount of I/S the peak separates becoming two interfering peaks where KI increases slower and Wv decreases quicker than in the previous stage.

Counting statistics: As Wv is the ratio of the heights at 10 Å and 10.5 Å, the value of Wv will be greatly changed by measuring errors. It is helpful to use the following expression (KLUG and ALEXANDER, 1974) for judging the error level of the two measurements:

$$100\sigma = 100\sqrt{M(M+1)/Np}/(M-1) \qquad (22)$$

where Np is the counts at maximum height, where measurements are made (including background), M is the ratio of the total counting rate at that maximum peak height to the background counting rate, and σ describes the standard deviation in the net height. It can be seen that a high background can reduce the accuracy. Therefore poor peak intensity and a high background will greatly decrease the accuracy in values which are dependent on the two heights at 10 Å and 10.5 Å, especially the latter. Since a narrow peak always results in a low value for the peak height at 10.5 Å and a relatively high background, the errors of the Wv for these narrow peaks are potentially large. These narrow peaks can only be used in figure 4 (A–F) to analyse the states of lattice strain if measuring statistics are known. Only where errors from both heights is less than 5% (eq. 22) can Wv be used to evaluate the state of domain size and lattice strain, and the presence of I/S.

The Weaver index (Wv) is actually controlled by two factors: the width of peak profile and its shape. With the same half-height width and different profile shapes of curves the Weaver index has different values. On one hand, this gives values of Wv a relatively large range of variation when compared with the Kübler index (KI). On the other hand, however, the Wv not only reflects the changes in the peak width but also indicates the changes of peak shape which, in turn, contains important information on the lattice strain of the sample (LANGFORD, 1978). Hence, Wv is better than the Kübler index for indicating variations in lattice strain. However the Weaver index is difficult to measure when the peak becomes very narrow (KÜBLER, 1968). Comparisons of BLENKINSOP'S (1988) empirical formulae relating the Kübler index and Weaver index with equations 1 and 3 reveal that the "power law" is close to the relationship between Weaver index and Kübler index described by equation 3 (this study), and the "exponential law" in most cases goes beyond this relationship (see Fig. 1). Since either the "exponential law" or the"power law" gives a large variation for both Wv and KI (Wv = 13–44 when KI = 0.1 °Δ2θ; KI = 0.17–0.4 °Δ2θ when Wv = 10, for instance, see Fig. 1) the uncertainty makes them difficult to use.

The Weber index describes the width of the 10 Å reflection of illite as the result of instrumental broadening (calibrated by the (100) reflection of quartz) hence, it is a comparable interlaboratory technique. However, the internal quartz standard must be larger than 3000 Å in mean size (from which the quartz reflection (100) is c. 0.14 °Δ2θ in half-width, this study) according to KLUG and ALEXANDER (1974). Comparisons of the empirical formulae relating the Kübler index and the Weber index (BLENKINSOP, 1988) with equations 13 show slightly different linear relationships (Fig. 3). Comparisons of Blenkinsop's relationship between the Weaver index and the Weber index with equations 7 and 9 are given in figure 2, from which it is seen that Blenkinsop's empirical formula is close to equation 9 of the Lorentzian curve relationship and with some extensive asymmetry (see section on asymmetric effect). However Blenkinsop's empirical formula relating Wv to Wb is only valid for the asymmetric case it fitted, and errors, sometimes large, will occur if it is used for other asymmetric or symmetric cases.

Summary and conclusions

An XRD peak can be characterised by five basic elements: position (d-spacing), maximum height, half-width, shape and asymmetry. The Kübler index reflects the half width of the 10 Å illite peak, i.e. the Scherrer width. The Weber index expresses this basic parameter normalised to the (100) reflection of a quartz standard. The Weaver index indicates the intensity variation at the peak maximum and 10.5 Å of the first illite basal reflection. Since the intensity at 10.5 Å is sensitive to shape changes of the 10 Å peak and influenced by the presence of I/S, the Weaver index contains information about the maximum and the shape of the 10 Å peak as well as information as to whether I/S is present. The Gaussian, the Lorentzian and the Pearson VII functions describe well, all these characteristics and the variations of the XRD peak. Linking the three IC indices the Kübler index, the Weaver index and the Weber index, with the Gaussian, Lorentzian and Pearson VII functions offers much new information about these IC indices.

All three indices of illite crystallinity, the Weaver index, the Kübler index and the Weber index, possess a sound basis in crystallography and an exact mathematical relationship exists between each of them. These relationships are flexible, comprehensive and precise. The plot of the relationship between the Kübler index and Weaver index offers a convenient and rapid method for the qualitative analysis of the domain size, the degree of lattice strain in illite, and for evaluating the presence of I/S.

Acknowledgements

The authors thank R.J. Merriman and A.H.N. Rice for reviewing the manuscript of this paper and their constructive suggestions. Thanks are also given to H.J. Kisch, L.N. Warr and A.H.N. Rice for kindly offering the IC sets. Callum Hetherington and R.J. Merriman revised the English. This research was supported by WZF Funds no–071094 and National Natural Science Foundation of China no–49872033.

References

ALEXANDER, L. (1948): Geometrical factors affecting the contours of X-ray spectrometer maxima. I. Factors causing asymmetry. J. Appl. Phys., 19, 1068–1071.

BALZAR, D. and LEDBETTER, H. (1993): Voigt-function modelling in fourier-analysis of size-broadened and strain-broadened X-ray-diffraction peaks. J. Appl. Cryst., 26, 97–103.

BALZAR, D. and POPOVIC, S. (1996): Reliability of the simplified integral-breadth methods in diffraction line-broadening analysis. J. Appl. Cryst., 29, 16–23.

BLENKINSOP, T.G. (1988): Definition of low-grade metamorphic zones using illite crystallinity. J. Metamorphic Geol., 6, 623–636.

DELHEZ, R., DE KEIJSER, TH., LANGFORD, J.I., LOUER, D., MITTERNEIJER, E.J. and SONNEVELD, E.J. (1993): Crystal imperfection broadening and peak shape in the Rietveld method. In: YOUNG, R.A. (ed.): The Rietveld Method, pp. 132–166. Oxford University Press, New York.

DRITS, V.A., EBERL, D.D. and SRODON, J. (1998): XRD measurement of mean thickness, thickness distribution and strain for illite and illite-smectite crystallites by the Bertaut-Warren-Averbach technique. Clays and Clay Minerals, 46, 38–53.

FREY, M. (1987): Very low-grade metamorphism of clastic sedimentary rocks. In: FREY, M. (ed.): Low Temperature Metamorphism, 9–58. Blackie and Son Ltd, Glasgow.

HALDER, N.C. and WAGNER, C.N.J. (1966): Separation of particle size and lattice strain in integral breadth measurement. Acta Cryst., 20, 312–313.

HOWARD, S.A. and PRESTON, K.D. (1989): Profile fitting of powder diffraction patterns. In: BISH, D.L. and POST, J.E. (eds): Modern Powder Diffraction. Reviews in Mineralogy, 20, 217–275. Mineral. Soc. Amer., Washington, D.C.

JIANG, W.-T., PEACOR, D.R., ÁRKAI, P., TOTH, M. and KIM, J.W. (1997): TEM and XRD determination of crystallite size and lattice strain as a function of illite crystallinity in pelitic rocks. J. Metamorphic Geol., 15, 267–281.

JONES, R.C. (1981): X-ray diffraction line analysis vs phosphorus sorption by 11 Puerto Rican soils. Soil Sci. Soc. Am. J., 45, 818–825.

JONES, F.W. (1938): The measurement of particle size by the X-ray method. Proc. Roy. Soc. (London), 166A, 16–42.

KISCH, H.J. (1991): Illite crystallinity: recommendations on sample preparation, X-ray diffraction settings, and interlaboratory samples. J. Metamorphic Geol. 9, 665–670.

KLUG, H.P. and ALEXANDER, L.E. (1974): X-ray Diffraction Procedures, 2nd ed. Wiley, New York.

KÜBLER, B. (1964): Les argiles, indicateurs de métamorphisme. Revue de l'Institut Français du Pétrole, 19, 1093–1112.

KÜBLER, B. (1968): Évaluation quantitative du métamorphisme par la cristallinité de l'illite. Bull. Centre Recherche Pau-SNPA, 2, 385–397.

LANGFORD, J.I. (1978): A rapid method for analysing the breadths of diffraction and spectral lines using the Voigt function. J. Appl. Crystal., 11, 10–14.

LANGFORD, J.I. (1992): Accuracy in powder diffraction II. In: PRINCE, E. and STALCK, J.K. (eds): NIST special publication no. 846, pp. 110–126. National Institute of Standards and Technology, Washington, D.C.

LANGFORD, J.I., LOUER, D., SONNEVELD, E.J. and VISSER, J.W. (1986): Applications of total pattern fitting to a study of crystallite size and strain in zinc oxide powder. Powder Diffraction, 1, 211–221.

LUDWIG, V. (1972): Die Paragenese Chlorit, Muscovit, Paragonit und Margarit im 'Griffelschiefer' des Ordoviziums in NE-Bayern (mit einem Beitrag zum Problem der Illit-Kristallinität). N. Jb Geol. Paläont. Mh, 9, 546–560.

MERRIMAN, P.J. and PEACOR, D.R. (1999): Very low-grade metapelites: mineralogy, microfabrics and measuring reaction progress. In: FREY, M. and ROBINSON, D. (eds): Low-Grade Metamorphism, pp. 10–60. Blackwell, Oxford.

NANDI, R.K. and SEN GUPTA, S.P. (1978): The analysis of X-ray diffraction profile from imperfect solids by an application of convolution relations. J. Appl. Cryst., 11, 6–9.

RIETVELD, H.M. (1969): A profile refinement method for nuclear and magnetic structures. J. Appl. Cryst., 2, 65–71.

RIETVELD, W. (1993): The early days: a retrospective view. In: YOUNG, R.A. (ed.): The Rietveld Method, pp. 39–42. Oxford University Press, New York.

RULAND, W. (1968): The separation of line broadening effects by means of line-width relations. J. Appl. Cryst., 1, 90–101.

SAVITZKY, A. and GOLAY, M.J.E. (1964): Smoothing and differentiation of data by simplified least squares procedures. Anal. Chem., 36, 1627–1639.

SCHERRER, P. (1918): Bestimmung der Grösse und der inneren Struktur von Kolloidteilchen mittels Röntgenstrahlen. Göttinger Nachr. Math. Phys., 2, 98–100.

SCHOENING, F.R. (1965): Strain and particle size values from X-ray line breadths. Acta Cryst., 18, 975–976.

WANG, H. and ZHOU, J. (1998): On the indices of illite crystallinity. Acta Petrol. Sinica, 14, 395–405.

WANG, H., FREY, M. and STERN, W.B. (1996): Diagenesis and metamorphism of clay minerals in the Helvetic Alps of eastern Switzerland. Clays and Clay Minerals, 44, 96–112.

WARR, L.N. and RICE, A.H.N. (1994): Interlaboratory standardization and calibration of clay mineral crystallinity and crystallite size data. J. Metamorphic Geol., 12, 141–152.

WARREN, B.E. and AVERBACH, B.L. (1952): The separation of cold-work distortion and particle size broadening in X-ray patterns. J. Appl. Phys., 33, 497.

WARREN, B.E. (1959): X-ray study of deformed metals. Progress in metal physics 8, pp. 147–202. Pergamon Press, London.

WEAVER, C.E. (1960): Possible use of clay minerals in search for oil. Bull. Amer. Assoc. Petroleum Geologists, 44, 1505–1518.

WEBER, K. (1972): Note on the determination of illite crystallinity. N. Jb. Mineral. Mh. 6, 267–276.

Manuscript received February 12, 1999; revision accepted March 28, 2000.

Erratum

The relationships between the Kübler index, Weaver index and Weber index of illite crystallinity and their applications

by *Hejing Wang* and *Jian Zhou*

Schweiz. Mineral. Petrogr. Mitt. 80/2, 187–198

p. 189, Tab. 1
to be replaced by correct version

Tab. 1 Contents and detail information of constants C_1 to C_{14}.

Constants	*Content*	*Note*
C_1	$2x(\ln 2)^{0.5}$	$x = 0.422\ \Delta°2\theta$, CuK$\alpha$
C_2	$\exp(C_1^2)$	
C_3	$2x$	
C_4	C_3^2	
C_5	$2x\,(2^{1/u}-1)^{0.5}$	$u = 1 \sim \infty$
C_6	C_5^2	
C_7	$C_1\,C_{14}$	
C_8	$C_2\,C_{14}^2$	
C_9	$C_3\,C_{14}$	
C_{10}	$C_4(C_{14})^2$	
C_{11}	$C_5\,C_{14}$	
C_{12}	$C_6(C_{14})^2$	
C_{13}	$1/C_{14}$	
C_{14}	$100/B_{100}^{Q}$	$B_{100}^{Q} = 0.14\ °2\theta$

p. 189. *Replace text in right column by*

The relationships between Kübler index (KI) and Weaver index (Wv) is given for the Gaussian curve by:

$$KI = C_1 / (\ln Wv)^{1/2} \quad (1)$$

$$Wv = (C_2)^{KI^{-2}} \quad (2)$$

for the Lorentzian curve by:

$$KI = C_3 / (Wv - 1)^{1/2} \quad (3)$$

$$Wv = C_4\,KI^{-2} + 1 \quad (4)$$

for the Pearson (VII) curve by:

$$KI = C_5 / (Wv^{1/u} - 1)^{1/2},\ u = 1 \sim \infty \quad (5)$$

$$Wv = (1 + C_6\,KI^{-2})^{u},\quad u = 1 \sim \infty \quad (6)$$

where C_1, C_2, C_3, C_4, C_5 and C_6 are constants and their values are listed in table 1. Figure 1 is a plot of the six equations and is called the KI–Wv plot.

The relationships between the Weaver index (Wv) and Weber index (Wb) are given for the Gaussian curves by:

$$Wb = C_7 / (\ln Wv)^{1/2} \quad (7)$$

$$Wv = (C_8)^{Wb^{-2}} \quad (8)$$

for the Lorentzian curve by:

$$Wb = C_9 / (Wv - 1)^{1/2} \quad (9)$$

$$Wv = C_{10}\,Wb^{-2} + 1 \quad (10)$$

Vorschau auf kommende Artikel

Evidence for Lower Paleozoic magmatism in the eastern Southalpine basement: zircon geochronology form Comelico porphyroids.
Sandro Meli and Urs S. Klötzli

Structural effects of OH => F substitution in trioctahedral micas of the system: K_2O-FeO-Fe_2O_3-Al_2O_3-SiO_2-H_2O-HF.
B. Boukili, J.L. Robert, J.-M. Beny and F. Hotz

Permian metabasalt and Triassic alkaline dykes in the northern Ivrea zone: clues to the post-Variscan geodynamic evolution of the Southern Alps.
V. Stähle

The crystal chemistry of the sartorite group minerals from Lengenbach, Binntal, Switzerland – a HRTEM study.
Allan Pring

Tectonic setting of the Internal Liguride units from central Liguria, Italy: new constraints from white mica and chlorite mineralogical studies.
A. Ellero, L. Leoni, M. Marroni and F. Sartori

Tectono-metamorphic evolution of the Simano-Adula nappe boundary, Central Alps, Switzerland.
Roger Rütti

(Änderungen vorbehalten)